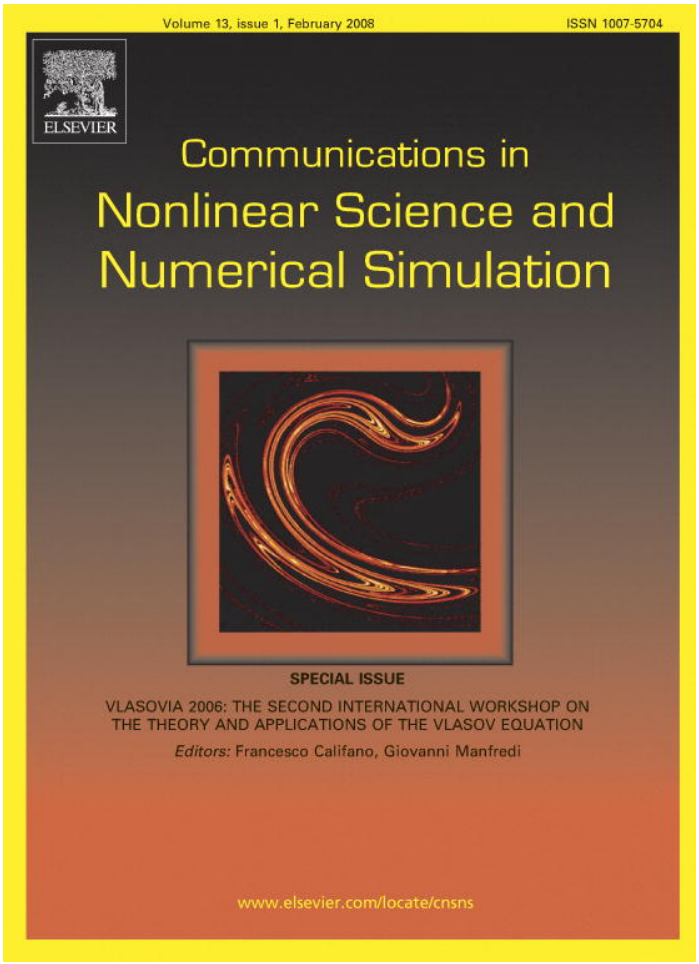

Available online at www.sciencedirect.com
ScienceDirect
Communications in Nonlinear Science and Numerical Simulation 13 (2008) 215–220
Communications in Nonlinear Science and Numerical Simulation
www.elsevier.com/locate/cnsns

Decay instability of electron acoustic waves

F. Valentini [a,b,*], T.M. O'Neil [b], D.H.E. Dubin [b]

[a] Dipartimento di Fisica and CNISM, Universitá della Calabria, Italy
[b] Physics Department, University of California at San Diego, California, USA

Available online 18 April 2007

Abstract

Eulerian and particle in cell (PIC) simulations are used to investigate the decay instability of electron acoustic waves (EAWs). An EAW is a nonlinear wave with a carefully tailored trapped particle population, that can be excited by a relatively low driver amplitude, if the driver is applied resonantly over many trapping periods. The excited EAW rings at nearly constant amplitude long after the driver is turned off, provided the EAW has the longest wavelength that fits in the plasma. Otherwise, the EAW decays to a longer wavelength EAW, through a vortex-like trapped particle population merging.

PACS: 52.65.Ff; 52.65.Rr; 52.35.Fp; 52.35.Mw; 52.35.Sb

Keywords: Vlasov; Eaw; Decay; Trapping

1. Introduction

In 1991, Hollway and Dorning [1] noted that certain nonlinear wave structures can exist in a plasma even at low amplitude. They called these waves electron acoustic waves (EAW) since the dispersion relation is of the acoustic form (i.e. $\omega = 1.31kv_{\text{th}}$ for small k). Here, ω is the angular frequency of the wave, k the wave number, and v_{th} the thermal velocity of the plasma electrons. Within linear theory, an EAW would be heavily Landau damped, since the wave phase velocity is comparable to the electron thermal velocity [2]. However, the EAW is a Bernstein–Green–Kruskal nonlinear mode (BGK mode) [3] with electrons trapped in the wave troughs. Because of the trapped electrons, the distribution of electron velocities is effectively flat at the wave phase velocity, and this turns off Landau damping.

As shown by the authors in [4], the EAWs can be launched by a small amplitude driver if the driver is applied resonantly over many trapping periods. The driver continuously replenishes the energy removed by Landau damping, so the trapped particle distribution (and the EAW) is eventually produced. This result

* Corresponding author. Address: Dipartimento di Fisica and CNISM, Universitá della Calabria, Italy. Tel.: +39 0984 496129; fax: +39 0984 494401.
E-mail address: valentin@fis.unical.it (F. Valentini).

1007-5704/$ - see front matter
doi:10.1016/j.cnsns.2007.04.012

was demonstrated using a particle in cell (PIC) simulation. For the case where the wavelength is the longest wavelength that fits in the plasma, the launched EAW persists at nearly constant amplitude long after the driver is turned off. However, when the driven EAW does not have the longest wavelength, the EAW decays to a longer wavelength EAW. In phase space, the trapped particles for an EAW appear to be a vortex structure, and the decay to longer wavelength involves a merger of the vortices [5–9]. In this sense the decay process can be thought as an example of inverse cascade.

In this paper, we first describe the excitation and decay of EAWs in a plasma with periodic boundary conditions. In this case, waves travel only in one direction as they would in an infinite length plasma (or a toroidal plasma). We then discuss the excitation and decay of EAWs in a plasma with particle and wave reflection at each end. In this case the EAWs are standing waves. In both cases, resonant excitation and decay to longer wavelength are observed.

2. Particle in cell simulation for a plasma with periodic boundary conditions

We scale time by the inverse plasma frequency ω_p^{-1}, where $\omega_p = \sqrt{4\pi ne^2/m}$ and n is the electron density. Length is scaled by the Debye length $\lambda_D = v_{th}/\omega_p$. With these choices, velocity is scaled by the electron thermal velocity $\lambda_D\omega_p = v_{th}$ and electric field by $\sqrt{4\pi nmv_{th}^2}$.

The PIC simulation follows the electron dynamics in the x-direction (the ions are considered motionless), which is the direction of wave propagation. The electron phase space domain for the simulation is $D = [0, L_x]\times[-v_{max}, v_{max}]$, where $v_{max} = 5$. For an initial set of simulations, we choose $L_x = 2\pi/k = 20$, but in later simulations the plasma length is increased to $L_x = 40$ and $L_x = 80$. This increase in length allows for decay to longer wavelength EAWs. The time step is $\Delta t = 0.1$. The simulations follow the evolution of $N \sim 5\times 10^6$–10^7 electrons for many plasma periods ($t_{max} = 4000$). The initial electron velocity distribution is taken to be Maxwellian. Periodic boundary conditions in physical space are imposed, and Poisson's equation is solved using a standard fast fourier transform (FFT) routine.

The external driver electric field is taken to be of the form $E_D(x,t) = E_D^{max}\{1 + [(t-\tau)/\Delta\tau]^n\}^{-1}\sin(kx - \omega t)$, where $E_D^{max} = 0.01$, $\tau = 1200$, $\Delta\tau = 600$, $n = 10$, and $k = \pi/10$. The plasma response is studied as a function of the driver frequency ω, or equivalently, phase velocity $v_\phi = \omega/k = 10\omega/\pi$. An abrupt turn on (or off) of the driver field would excite Langmuir waves as well as EAWs, complicating the analysis. Thus, the driver is turned on and off adiabatically. The driver amplitude is near E_D^{max} (within a factor of two) for several trapping periods [10] ($t_{off} - t_{on} \simeq 1200 \simeq 11\tau_D$), and is near zero again by $t_{off} = 2000$. Here, the trapping period associated with the maximum driver field is $\tau_D = 2\pi/\sqrt{kE_D^{max}} = 112$.

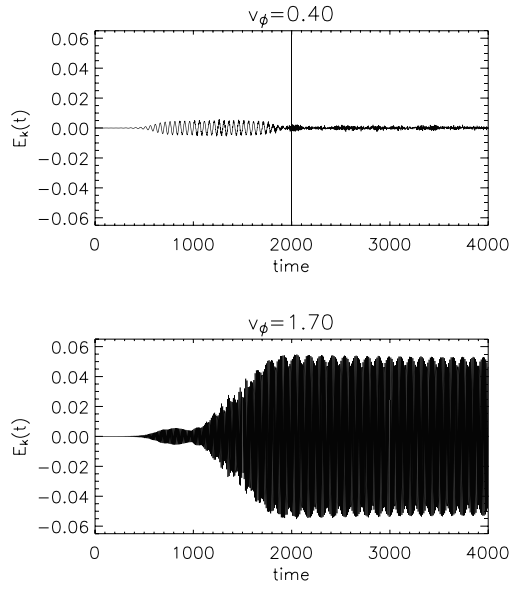

Fig. 1. Plasma response for two different values of the driver phase velocity: $v_\phi = 0.4$ (at the top) and $v_\phi = 1.70$ (at the bottom).

Fig. 1 shows the evolution of the plasma electric field, $E_k(t)$, for two different values of the driver phase velocity. In the top graph (for $v_\phi = 0.4$), $E_k(t)$ rises to a small value while the driver is on, but falls to zero when the driver is turned off. The time t_{off} is indicated by the dashed line. In the bottom graph (for

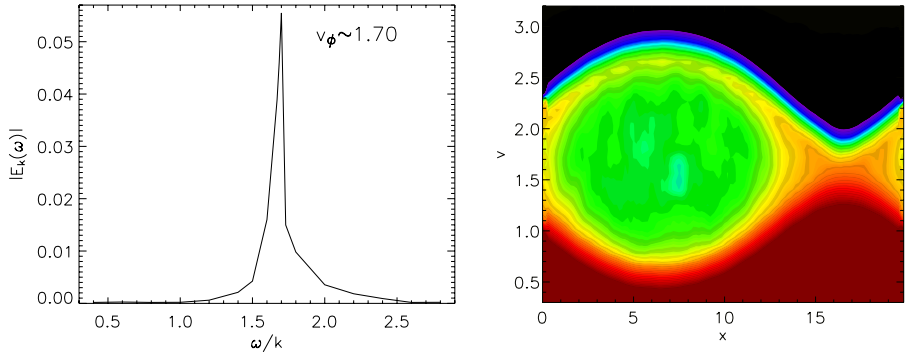

Fig. 2. Left panel: The peak of resonance for the EAW. Right panel: phase space contour plot of the distribution function f at $t = 4000$.

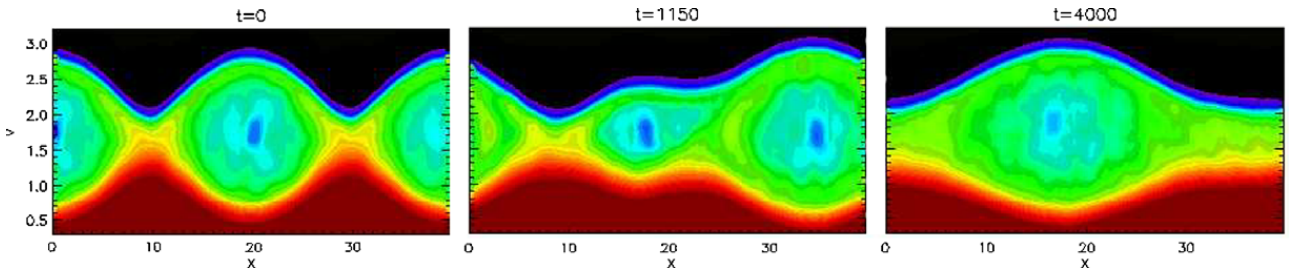

Fig. 3. The coalescence and merging of two phase space holes.

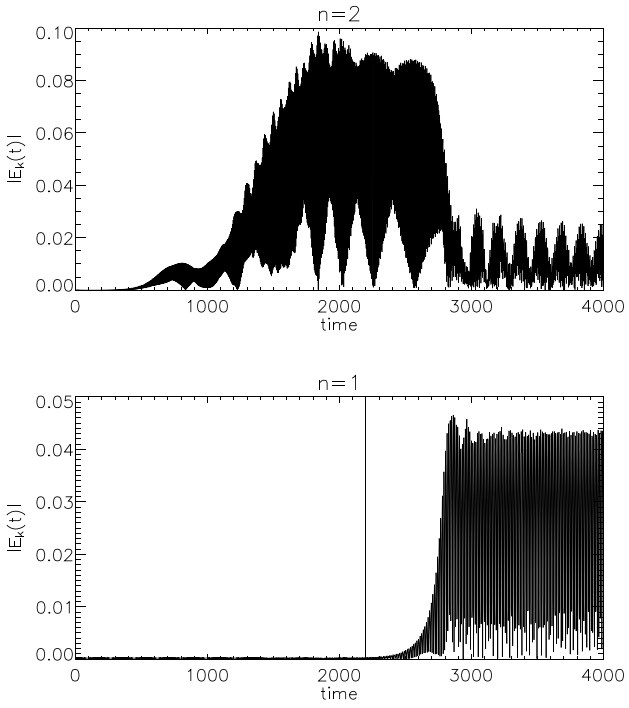

Fig. 4. Time evolution of the electric field spectral components $n = 2$ and $n = 1$.

$v_\phi = 1.70$), $E_k(t)$ grows to large amplitude and maintains this amplitude (rings) after the driver is turned off. Repeating such simulations for many different phase velocities (but holding the other driver parameters fixed at the values listed) yields the peaked graph in Fig. 2 (left panel). Here, the ordinate is the amplitude of the oscillating plasma electric field at the end of the simulation (long after the driver has been turned off), and the abscissa is the driver phase velocity. For this set of driver parameters, an EAW is driven resonantly for phase velocity $v_\phi \simeq 1.70$. As discussed in [4], the value of the resonant phase velocity is shifted upward due to finite amplitude effects.

The mode has a population of trapped particles and is properly a BGK mode as discussed in [4]. Fig. 2 (right panel) shows a false color contour plot of the electron distribution, $f(x,v)$, at the end of the run ($t = 4000$). The color code assigns higher values of f to longer wavelengths in spectrum. The vortex-like structure in the figure represents trapped particles, and as expected these particles have a mean velocity equal to the phase velocity $v\phi = 1.7$.

The EAW in the bottom graph of Fig. 1 rings at nearly constant amplitude after the driver is turned off. However, the wavelength for this mode is the longest wavelength that fits in the simulation domain, so the constant amplitude is no guarantee against decay to a longer wavelength mode. Moreover, previous theory suggested that BGK modes with trapped particles may be subject to such decay instabilities [5–9]. To investigate the possibility of decay to a longer wavelength mode, we replicate the mode periodically in space and use it as the initial condition for a simulation in a longer domain. The matching from wavelength to wavelength is smooth since periodic boundary conditions were used in the initial simulation.

Fig. 3 shows a temporal sequence of phase space contours for the case where the simulation domain has been doubled in length ($L_x = 20 \rightarrow L_x = 40$). The contour plot for $t = 0$ is simply two copies of the plot in Fig. 2 (right panel) placed side by side. The $t = 0$ plot shows two vortex-like structures representing trapped particles. The sequence of plots shows a progressive merger of the two vortices until there is only a single vortex at $t = 4000$. A decay instability has transferred the energy from mode 2 (i.e. $k = 2 \cdot 2\pi/40 = \pi/10$), to mode 1 (i.e. $k = 1 \cdot 2\pi/40 = \pi/20$); that is, to the longest wavelength that fits in the simulation domain. Also, we have carried out simulations for $L_x = 80$ (4 initial vortices) and again observed merger to a single vortex (see Ref. [4] for more details). From these observations, we expect that merger to a single vortex (or decay to the longest mode) is a general tendency for EAWs. This is consistent with observations for the merger of phase space vortices in other situations, such as the vortical holes that result from the two stream instability [5–9].

3. Eulerian Vlasov simulation for a plasma with particle and wave reflection at each end

For the above simulations, with periodic boundary conditions at each end, the EAWs all travel in the same direction. However, for a straight finite length plasma column, particles and waves undergo reflection at each end, and the EAWs of interest are standing waves. One might worry that the nonlinear trapped particle distributions traveling in opposite direction would interfere and spoil the excitation and decay results obtained for the traveling EAWs. To see that the results persist for standing EAWs, we carried out simulations with particle reflection at each end (i.e. at $x = 0$ and $x = L_x$). The wave electric field is required to be zero at each end, as is appropriate for matching on to the vacuum field beyond the end of the column [11].

We can model this situation (specular particle reflection at each end and zero wave electric field at each end) by using a simulation with periodic boundary conditions on a domain that is twice the length of the plasma [i.e. $D = [0, L_{max} = 2L_x]$]. The driver field and all plasma noise must be such as to maintain zero electric field at $x = 0$ and $x = L_x$. The numerical integration of the Vlasov equation is based on the splitting scheme [12] (an Eulerian code), while a standard FFT is used to integrate Poisson equation in the periodic domain $D = [0, 2L_x]$.

The initial distribution function is a Maxwellian in velocity space, over which a noise modulation in the physical space with amplitude $A_{noise} = 10^{-4}$ is superposed $f(x, v, t = 0) = 1/\sqrt{2\pi}e^{-\frac{v^2}{2}}[1 + A_{noise}\sum_{j=0}^{j_{max}} \cos(k_j x)]$, where $j_{max} = 20$, $k_j = jk_0$ and $k_0 = 2\pi/L_{max}$ represents the fundamental wave number in the simulation box. The simulation domain in phase space is given by $D = [0, L_{max}] \times [-v_{max}, v_{max}]$, where $v_{max} = 6$. Outside the velocity simulation interval the distribution function is put equal to zero. Typically a simulation is performed using $N_x = 512$ grid points in the physical space and $N_v = 2400$ grid points in the velocity space and the time step is $\Delta t = 0.001$.

To excite the electron acoustic wave, we use an external driver electric field (in this case, a standing wave in the simulation domain), taken to be of the form $E_D(x,t) = E_D^{max}\{1 + [(t-\tau)/\Delta\tau]^{\beta}\}^{-1}[\sin(nk_0x - \omega t) + \sin(nk_0x + \omega t)]$, where $E_D^{max} = 0.01$, $\tau = 1200$, $\Delta\tau = 600$, $\beta = 10$, and $n = 2$ (we drive the mode $n = 2$). We choose a simulation domain of total length $L_{max} = 2L_x = 40$, but all the results will be presented for $0 < x < L_x = 20$, that is the actual length of the plasma confined in the trap. In these conditions, the resonant phase velocity for the electron acoustic waves is $v_\phi = \omega/(nk_0) \simeq 1.70$, as discussed earlier.

The time evolution of the electric field spectral component $n = 2$ and $n = 1$ is displayed in Fig. 4. The mode $n = 2$ is excited during the driving process; a big plasma response is observed around $t = 1000$, and the perturbation amplitude grows while the driver pumps energy into the system, then the electric field reaches a constant saturation value at $t \simeq 1800$ and goes on oscillating around the saturation value until the driver is turned off at $t = 2200$. Then the decay instability transfers energy from the mode $n = 2$ to the mode $n = 1$ (i.e. to the largest wavelength that fits in the simulation box). The dashed line in the bottom graph in Fig. 4 represents the time $t = t_{off}$; it is easily seen that the mode $n = 1$ starts growing for $t > t_{off}$, then saturates and rings at nearly constant amplitude, for many wave cycles. Obviously, the phase of the noise determines the phase of the daughter wave in the decay instability. Since the electric field must be zero at the ends of the plasma, we admit only standing wave noise components with zero field at the ends of the column. In a real finite length plasma only such noise components would be significant because of the requirement that the field in the plasma match onto vacuum fields beyond the end of the column [11]. The value of the electric field at $x = 0$ and $x = L_x$ remains smaller than 10^{-10} until the end of the simulation. We point out that with a PIC code it is harder to control the phase of the daughter wave. In fact, the statistical noise due to the finite number of particles in a PIC simulation makes the daughter wave have a phase different from that of the initial sine wave.

Finally, the decay instability has been analyzed looking at the contour plot of the electron distribution function in phase space. In Fig. 5, the level lines of the distribution are shown for several times after the driver is turned off. At the beginning, two vortex structures are visible in phase space, the first moving with positive velocity $v = v_\phi \simeq 1.7$ along the x axis and the other one moving with $v = -v_\phi$. Each of them bounces back and forth in the trap, corresponding to a circular motion in phase space, as it can be seen from the figure. During the decay instability the two vortices merge, and finally one big vortex is present in the trap that still bounces back and forth, being reflected at the two ends.

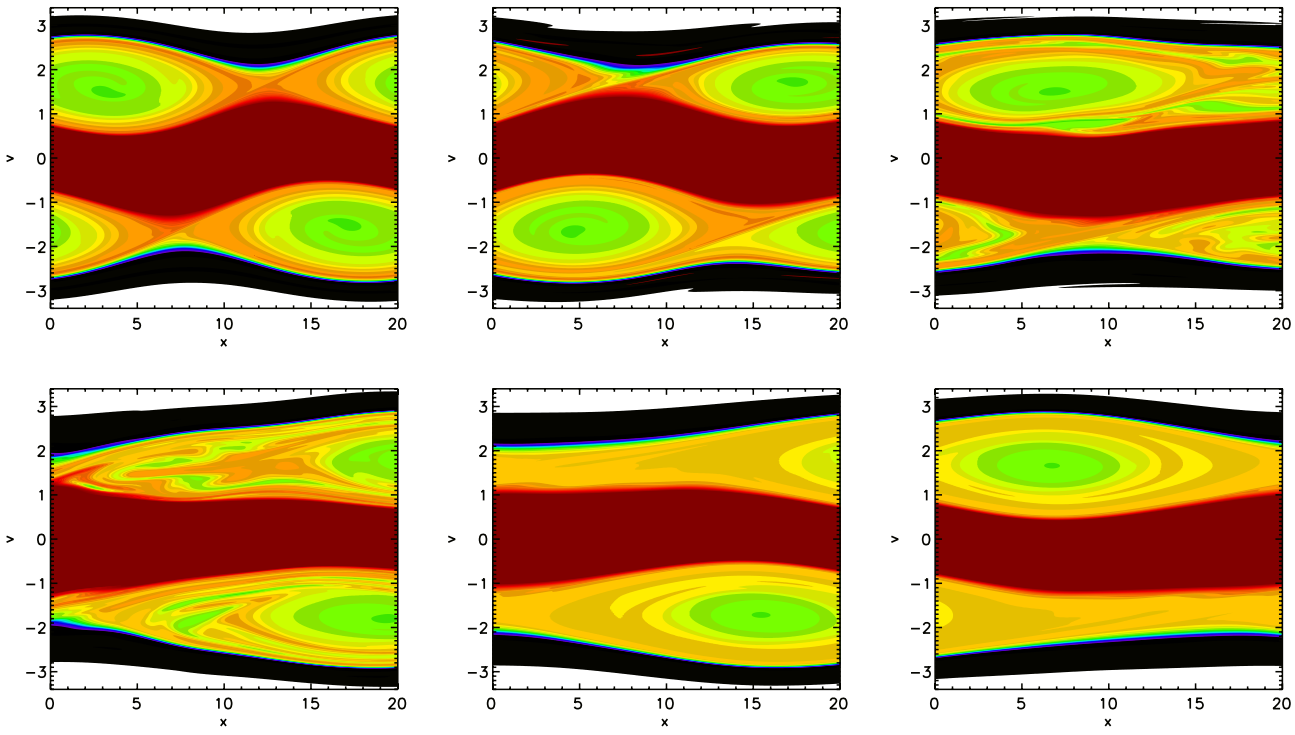

Fig. 5. Contour plot of the distribution function in phase space, for $t > 2200$.

References

[1] Holloway JP, Dorning JJ. Phys Rev A 1991;44:3856.
[2] Landau LD. J Phys (Moscow) 1946;10:25.
[3] Bernstein IB, Green JM, Kruskal MD. Phys Rev Lett 1957;108:546.
[4] Valentini F, O'Neil TM, Dubin DHE. Phys Plasmas 2006;13:052303.
[5] Berk HL, Nielsen CE, Roberts KV. Phys Fluids 1970;13:980.
[6] Ghizzo A, Izrar B, Bertrand P, Fijalkov E, Feix MR, Shoucri M. Phys Fluids 1988;31:72.
[7] Manfredi G, Bertrand P. Phys Plasmas 2000;7:2425.
[8] DePackh DC. J Electron Control 1962;13:417.
[9] Dory RA. J Nucl Energy Pt C 1964;6:511.
[10] O'Neil T. Phys Fluids 1965;8:2255.
[11] Prasad SA, O'Neil TM. Phys Fluids 1983;26:665.
[12] Cheng CZ, Knorr G. J Comput Phys 1976;22:330–51.